Nur77 serves as a molecular brake of the metabolic switch during T cell activation to restrict autoimmunity

Marie Liebmann[a,1], Stephanie Hucke[a,1], Kathrin Koch[a], Melanie Eschborn[a], Julia Ghelman[b], Achmet I. Chasan[c], Shirin Glander[d], Martin Schädlich[d], Meike Kuhlencord[c], Niklas M. Daber[c], Maria Eveslage[e], Marc Beyer[f,g], Michael Dietrich[h], Philipp Albrecht[h], Monika Stoll[d], Karin B. Busch[i], Heinz Wiendl[a], Johannes Roth[c], Tanja Kuhlmann[b], and Luisa Klotz[a,2]

[a]Department of Neurology with Institute of Translational Neurology, University Hospital Muenster, 48149 Muenster, Germany; [b]Institute of Neuropathology, University Hospital Muenster, 48149 Muenster, Germany; [c]Institute of Immunology, University of Muenster, 48149 Muenster, Germany; [d]Department of Genetic Epidemiology, Institute of Human Genetics, University of Muenster, 48149 Muenster, Germany; [e]Institute of Biostatistics and Clinical Research, University of Muenster, 48149 Muenster, Germany; [f]Department of Genomics and Immunoregulation, Life and Medical Sciences Institute, University of Bonn, 53115 Bonn, Germany; [g]Molecular Immunology, German Center for Neurodegenerative Diseases, 53127 Bonn, Germany; [h]Department of Neurology, University of Düsseldorf, 40225 Düsseldorf, Germany; and [i]Institute for Molecular Cell Biology, University of Muenster, 48149 Muenster, Germany

Edited by Jason G. Cyster, University of California, San Francisco, CA and approved July 6, 2018 (received for review December 4, 2017)

T cells critically depend on reprogramming of metabolic signatures to meet the bioenergetic demands during activation and clonal expansion. Here we identify the transcription factor Nur77 as a cell-intrinsic modulator of T cell activation. Nur77-deficient T cells are highly proliferative, and lack of Nur77 is associated with enhanced T cell activation and increased susceptibility for T cell-mediated inflammatory diseases, such as CNS autoimmunity, allergic contact dermatitis and collagen-induced arthritis. Importantly, Nur77 serves as key regulator of energy metabolism in T cells, restricting mitochondrial respiration and glycolysis and controlling switching between different energy pathways. Transcriptional network analysis revealed that Nur77 modulates the expression of metabolic genes, most likely in close interaction with other transcription factors, especially estrogen-related receptor α. In summary, we identify Nur77 as a transcriptional regulator of T cell metabolism, which elevates the threshold for T cell activation and confers protection in different T cell-mediated inflammatory diseases.

Nur77 | immunometabolism | autoimmunity | T cells

Significance

The role of metabolic processes during T cell activation has been increasingly acknowledged, and recent data suggest an impact of T cell immunometabolism on T cell function and T cell-mediated autoimmunity. The factors regulating metabolic function in T cells are not clear, however. We identify the nuclear receptor Nur77 as central regulator of T cell immunometabolism, controlling oxidative phosphorylation and aerobic glycolysis during T cell activation. Functionally, Nur77 restricts murine and human T cell activation and proliferation and limits inflammation in autoimmune conditions in animal models of CNS autoimmunity, contact dermatitis, and arthritis. These findings identify Nur77 as a central regulator of T cell immunometabolism that restricts T cell-mediated autoimmunity, which might open up new avenues for a more tailored therapeutic approach.

Autoimmune diseases, such as lupus erythematosus, rheumatoid arthritis, and multiple sclerosis (MS), affect 5–8% of the worldwide population and occur when a specific adaptive immune response is mounted against self-antigens (1, 2). These peripherally generated autoreactive T cells then infiltrate the respective target organs, where they are reactivated by their respective self-antigen presented by local antigen-presenting cells (APCs), resulting in local T cell expansion and inflammation (2).

Recent years have seen growing interest in understanding the metabolic processes underlying T cell activation and function. T cell metabolism is extremely dynamic, as T cells need to rapidly switch from a resting state to an activated state, which requires sufficient energy and building blocks for cell proliferation and acquisition of effector functions (3). While naive T cells have a low demand for energy and depend primarily on fatty acid oxidation and oxidative phosphorylation, activated effector T cells strongly increase glycolysis to serve their energy demands (4). In contrast, memory T cells exhibit an increased capacity for oxidative phosphorylation, which explains their energetic advantage underlying their rapid recall ability (5). Furthermore, there is growing appreciation that metabolic changes in fact shape the fate of T cells by providing distinct cues for differentiation into different T helper or regulatory cell subsets (6). These insights have led to the idea that targeted manipulation of immune cell metabolism might be a powerful tool to shape immune cell responses in different diseases, such as autoimmunity, vaccination, and antitumor immunity (7, 8). However, the clues how external signals are intracellularly translated into modulation of T cell metabolism and how metabolic processes in T cells are operated and regulated remain sparse.

Author contributions: M.L., S.H., P.A., M. Stoll, K.B.B., H.W., J.R., T.K., and L.K. designed research; M.L., S.H., K.K., M. Eschborn, J.G., A.I.C., M.K., N.M.D., and M.D. performed research; M.L., S.H., K.K., M. Eschborn, J.G., A.I.C., S.G., M. Schädlich, M.K., N.M.D., M. Eveslage, M.B., M.D., P.A., M. Stoll, J.R., T.K., and L.K. analyzed data; and M.L., S.H., and L.K. wrote the paper.

Conflict of interest statement: S.H. has received speaker honoraria from Novartis. M.E. has received speaker honoraria and travel support from Sanofi Genzyme. M.D. had received speaker honoraria from Novartis. P.A. has received compensation for serving on Scientific Advisory Boards for Ipsen, Novartis, and Biogen; speaker honoraria and travel support from Novartis, Teva, Biogen, Merz Pharmaceuticals, Ipsen, Allergan, Bayer Healthcare, Esai, UCB, and Glaxo Smith Kline; and research support from Novartis, Biogen, Teva, Merz Pharmaceuticals, Ipsen, and Roche. H.W. has received compensation for serving on Scientific Advisory Boards/Steering Committees for Biogen, Evgen, MedDay Pharmaceuticals, Merck Serono, Novartis, Roche Pharma, and Sanofi-Genzyme; speaker honoraria and travel support from Alexion, Biogen, Cognomed, F. Hoffmann-La Roche, Gemeinnützige Hertie-Stiftung, Merck Serono, Novartis, Roche Pharma, Sanofi-Genzyme, TEVA, and WebMD Global; compensation as a consultant from Abbvie, Actelion, Biogen, IGES, Novartis, Roche, Sanofi-Genzyme, and the Swiss Multiple Sclerosis Society; and research support from German Ministry for Education and Research, German Research Foundation, Else Kröner Fresenius Foundation, Fresenius Foundation, Hertie Foundation, North Rhine-Westphalia Ministry of Education and Research, Interdisciplinary Center for Clinical Studies Muenster, Rasmussen Encephalitis Children's Foundation, Biogen, GlaxoSmithKline, Roche Pharma, and Sanofi-Genzyme. L.K. has received compensation for serving on Scientific Advisory Boards for Genzyme and Novartis; speaker honoraria and travel support from Novartis, Merck Serono, Roche, Genzyme, and Biogen; and research support from Novartis and Biogen. T.K. has received honoraria for lecturing from Novartis, Merck Serono, Sanofi Aventis Bayer Health Care, and TEVA.

This article is a PNAS Direct Submission.

Data deposition: The data reported in this paper have been deposited in the Gene Expression Omnibus (GEO) database, https://www.ncbi.nlm.nih.gov/geo (accession no. GSE114912).

[1]M.L. and S.H. contributed equally to this work.

[2]To whom correspondence should be addressed. Email: luisa.klotz@ukmuenster.de.

This article contains supporting information online at www.pnas.org/lookup/suppl/doi:10.1073/pnas.1721049115/-/DCSupplemental.

Published online August 2, 2018.

Among others, the mechanistic target of rapamycin (mTOR) (9) and estrogen-related receptor-α (ERRα) (4) have been identified as intrinsic factors that modulate T cell responses by altering T cell metabolism. Nur77 (NR4A1), like ERRα, belongs to the superfamily of nuclear receptors, a large family of receptors that act as ligand-dependent or -independent transcription factors. Like its family members Nurr1 (NR4A2) and Nor1 (NR4A3), Nur77 is associated with a broad range of cellular processes, including proliferation, differentiation, apoptosis, metabolism, and inflammation, depending on tissue and context (10). Nur77 is an immediate–early response gene expressed in T cells within hours after T cell receptor (TCR) stimulation (11). It is also well-known for its role in thymic negative selection, where induction of Nur77 results in apoptosis of immature thymocytes (12, 13). As T cells that escape thymic negative selection can contribute to autoimmunity, Nur77 might be important for the control of autoreactive T cells during negative selection (14).

Here we investigated the role of Nur77 during early activation, proliferation, and acquisition of effector functions of murine and human T cells. We found that Nur77 is induced within hours after TCR stimulation, and that Nur77-deficiency in T cells leads to enhanced proliferation, differentiation, and cytokine production in vitro and in vivo. These effects on T cell activation could be linked to a combined control of mitochondrial respiration and aerobic glycolysis, due at least in part to transcriptional control of a range of metabolically relevant genes. Pathophysiologically, Nur77 plays a central role in T cell-mediated inflammatory diseases, as illustrated in different animal models of experimental autoimmune encephalomyelitis, contact dermatitis, and rheumatoid arthritis. Taken together, our findings identify Nur77 as a T cell-intrinsic factor that controls T cell metabolism and T cell-mediated inflammatory diseases.

Results

Nur77 Restricts Activation and Expansion of T Cells in Vitro and in Vivo. It has been reported that older Nur77^{KO} mice exhibit splenomegaly (15); however, the cellular origin and underlying mechanisms have not yet been addressed. In light of the acknowledged role of Nur77 in the context of apoptosis of immature thymic T cells, we evaluated cellular compositions of spleens from wild-type (WT) and Nur77^{KO} mice at different time points. Indeed, 30-wk-old Nur77^{KO} mice exhibited splenomegaly, with significantly increased numbers of splenocytes compared with WT mice (Fig. 1*A*), which was not observed in 6-wk-old mice (not shown). Flow cytometric analysis of splenic cellular subset composition revealed that Nur77^{KO} mice showed a significantly increased percentage of CD4$^+$ and CD8$^+$ T cells at age 30 wk (Fig. 1*B* and *SI Appendix*, Fig. S1*A*), but no alterations in the frequencies of CD19$^+$ B cells, CD11b$^+$ myeloid cells, and CD11c$^+$ dendritic cells (DCs) (*SI Appendix*, Fig. S1*B*). These results suggest that Nur77^{KO} T cells accumulate in adult mice in the absence of an exogenous stimulus.

Following this line of reasoning, we evaluated whether a lack of Nur77 in T cells promotes spontaneous T cell proliferation. Naive CD4$^+$ T cells isolated from Nur77^{WT}-OTII or Nur77^{KO}-OTII mice were transferred into Rag1^{KO} mice, which lack their own T and B cells, and homeostatic T cell proliferation was determined by flow cytometry after 10 d using the TCR-specific antibody Vβ5.2 for identification of transferred T cells. Importantly, a lack of Nur77 resulted in pronounced T cell proliferation (Fig. 1*C*), and these T cells expressed higher levels of CD44, a marker associated with memory T cells (*SI Appendix*, Fig. S1*C*). In a corresponding in vitro setup of homeostatic proliferation (16), proliferation of Nur77-deficient T cells (Nur77^{KO}-OTII) remained increased in the presence of blocking antibodies against the major histocompatibility complex II (MHC-II) and IL-7 (Fig. 1*D*), suggesting a cell autonomous effect. Further characterization of Nur77^{KO} mice revealed that CD4$^+$ T cells exhibited increased expression of the activation markers CD25 and CD69 at both 6 wk and 30 wk, as well as increased percentage of T cells with a memory phenotype (i.e., CD44^{hi} and CD62L^{low}) at both time points (Fig. 1*E* and *SI Appendix*, Fig. S1*D*). Similar findings for CD69 and memory cell markers (CD44 and CD62L) were observed for CD8$^+$ T cells at age 30 wk (*SI Appendix*, Fig. S1*E*). Taken together, our results point to a role for Nur77 in the restriction of T cell expansion and activation even in the absence of an inflammatory stimulus.

We next asked whether Nur77 might also play a role during T cell activation. Nur77 expression was induced within 2–4 h after initial CD4$^+$ T cell stimulation via the TCR and did not depend on additional costimulatory signals via αCD28 or the presence of polarizing cytokines facilitating Th1, Th17, and regulatory T cell (Treg) differentiation (Fig. 1*F* and *SI Appendix*, Fig. S1*F*). Since this suggests that Nur77 could be involved in the modulation of effector T cell responses, we hypothesized that Nur77 deficiency alters proliferation and cytokine production on activation. Indeed, stimulated Nur77^{KO} CD4$^+$ T cells exhibited significantly increased proliferation (Fig. 1*G*) and produced significantly enhanced amounts of effector cytokines IFN-γ and IL-17A compared with activated WT CD4$^+$ T cells (Fig. 1*H*). Also on antigen-specific activation, transgenic Nur77^{KO}-OTII and Nur77^{KO}-2D2 CD4$^+$ T cells proliferated more vigorously and produced significantly enhanced amounts of cytokines compared with their respective Nur77-competent transgenic controls (Fig. 1*I* and *SI Appendix*, Fig. S1*G*).

To examine the role of Nur77 in human CD4$^+$ T cells, we next assessed Nur77 expression in human CD4$^+$ T cells by immunocytochemistry and flow cytometry on αCD3-mediated activation (Fig. 1*J*), and again observed a rapid and transient up-regulation of Nur77 expression in T cells on stimulation. Importantly, siRNA-mediated knockdown of Nur77 expression in stimulated human CD4$^+$ T cells (Fig. 1*K* and *SI Appendix*, Fig. S1*H*) significantly elevated production of the proinflammatory cytokines IFN-γ, IL-17A, and GM-CSF (Fig. 1*L*). Furthermore, we observed significantly enhanced differentiation into IFN-γ–producing Th1 cells as well as IL-17A–producing Th17 cells on siRNA knockdown of Nur77 when CD4$^+$ T cells were also treated with polarizing cytokines (*SI Appendix*, Fig. S1*I*). Thus, our data identify Nur77 as an important regulator of CD4$^+$ T cells both under homeostatic conditions and on TCR-mediated stimulation, suggesting that Nur77 might be involved in the control of T cell responses potentially to impede the development of autoimmunity.

Nur77 Restricts T Cell-Mediated CNS Autoimmunity. To address this possibility in more depth, we crossed Nur77^{KO} mice (17) with 2D2 mice (18) to generate Nur77^{KO}-2D2 mice, because 2D2 mice are known to exhibit increased susceptibility to the development of spontaneous CNS autoimmunity due to the high frequency of CNS autoantigen-specific CD4$^+$ T cells, especially on introduction of a second disease-promoting transgene, such as *Tnfr2* or *Tob1* (19, 20). Importantly, a lack of Nur77 in 2D2 mice resulted in a significant increase in disease incidence and in the severity of clinical signs associated with CNS autoimmunity, as illustrated by the cumulative experimental autoimmune encephalomyelitis (EAE) score, which combines evaluation of tail tonus, ground gait, and hind leg clasping (*SI Appendix*, Fig. S2*A*). Nur77^{KO}-2D2 mice (n = 16) developed clinical signs earlier than Nur77^{WT}-2D2 mice (n = 15 mice), and exhibited significantly greater overall severity of clinical signs (Fig. 2*A* and *SI Appendix*, Fig. S2 *B–D*). This finding was confirmed in a second, independent cohort of mice (*SI Appendix*, Fig. S2*E*). The evaluation of clinical signs in mice predominantly reflects spinal cord involvement; however, spontaneous CNS autoimmunity on a 2D2 background also affects the optic nerves as a second predilection site (18). Therefore, we determined visual function by measuring the optokinetic tracking response. Interestingly, the aggravated disease severity in Nur77^{KO}-2D2 mice seems to be accompanied by increased vision impairment, although the difference between the two mouse strains did not reach statistical significance (Fig. 2*B*). In line with our clinical findings, histological analysis of spinal cord revealed that Nur77^{KO}-2D2 mice displayed increased lesion burden (Fig. 2*C*). In addition, increased numbers of CD4$^+$ T cells were detected in the CNS by flow cytometric analysis (Fig. 2*D*). Furthermore, ex vivo

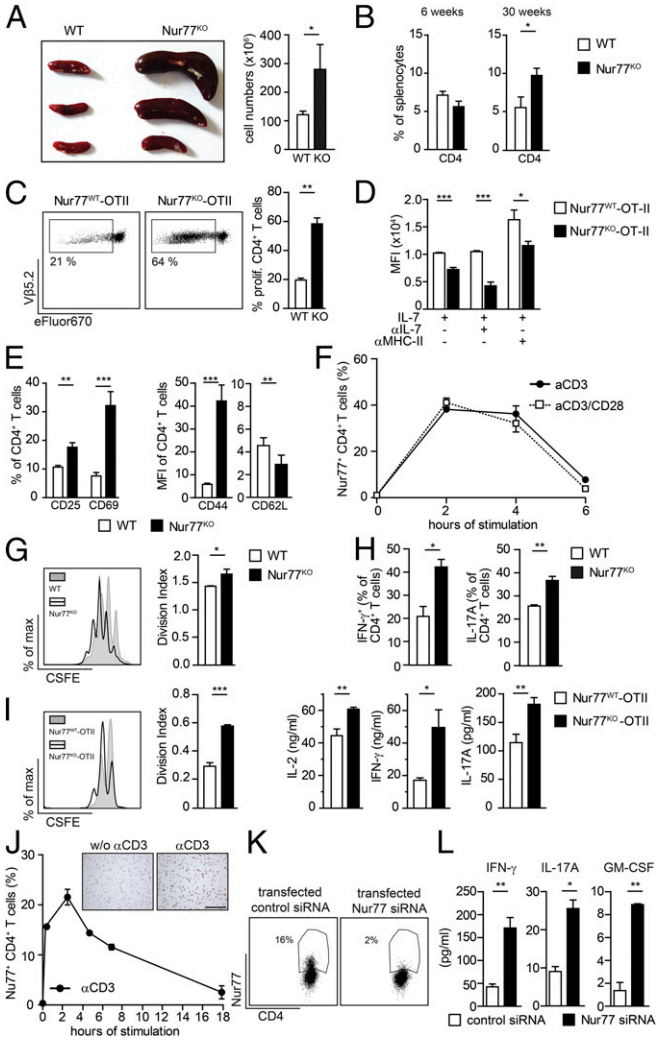

Fig. 1. Nur77 restricts proliferation and activation of T cells. (*A*) Appearances of spleens from 30-wk-old C57BL/6J and Nur77^{KO} mice. The graph displays total cell numbers; $n = 6$/group. (*B*) Frequency of splenic CD4$^+$ T cells was determined in 6- or 30-wk-old C57BL/6J or Nur77^{KO} mice by flow cytometry; $n = 6$/group. (*C*) Homeostatic T cell proliferation of eFluor670-labeled Nur77^{WT}-OTII and Nur77^{KO}-OTII T cells in Rag1^{KO} mice; $n = 7$–8/group. The mean percentage of proliferated splenic T cells was determined by flow cytometric analysis on day 10 after transfer. (*D*) Nur77^{WT}-OTII and Nur77^{KO}-OTII T cells were stimulated in an antigen-specific manner in the presence of 10 ng/mL IL-7 as well as blocking antibodies against MCH-II and IL-7 (both 5 μg/mL). After 6 d, T cells were labeled with eFluor670 and injected into Rag1^{KO} mice; $n = 2$/group. The mean fluorescence intensity (MFI) of proliferated T cells was determined by flow cytometric analysis on day 6 after transfer. (*E*) Surface expression of CD25 or CD69 (markers of early activation; *Left*) or CD44 and CD62L (markers of memory phenotype; *Right*) on splenic CD4$^+$ T cells from 30-wk-old C57BL/6J and Nur77^{KO} mice was analyzed by flow cytometry. The percentage of positive T cells or MFI is shown; $n = 6$/group. (*F*) Nur77 expression of αCD3/αCD28-stimulated WT CD4$^+$ T cells was determined by flow cytometry at the indicated time points. (*G*) CD4$^+$ T cell (C57BL/6J or Nur77^{KO}) proliferation on αCD3 stimulation was analyzed by flow cytometry after 72 h. Shown are representative histograms and division index. (*H*) WT and Nur77^{KO} CD4$^+$ T cells were subjected to Th1 (IFN-γ, *Left*) and Th17 (IL-17A, *Right*) conditions. Cytokine production on restimulation was assessed by flow cytometry after 72 h. (*I*) Nur77^{WT}-OTII or Nur77^{KO}-OTII T cells were cocultured with OVA$_{323–339}$–loaded DCs. After 72 h, proliferation (*Left*) and cytokine secretion (*Right*) were analyzed. (*J*) Nur77 expression was analyzed in αCD3-stimulated human CD4$^+$ T cells by immunohistochemistry after 4 h and flow cytometry at the indicated time points, respectively. (Scale bar: 200 μm.) (*K*) Human CD4$^+$ T cells were cotransfected with control-siRNA or Nur77-siRNA. Nur77 expression was analyzed in transfected CD4$^+$ T cells after αCD3 stimulation for 3 h. Representative dot plots are shown. (*L*) Cytokine production of transfected and αCD3 ± αCD28-stimulated CD4$^+$ T cells was analyzed by ELISA after 72 h. Graphs display mean ± SEM of one representative experiment of three experiments, unless stated otherwise. Statistical analysis was performed using Student's *t* test. $*P \le 0.05$; $**P \le 0.001$; $***P \le 0.001$.

restimulation of CNS-derived CD4$^+$ T cells showed that Nur77-deficient CD4$^+$ T cells produced significantly more IFN-γ than their Nur77-competent counterparts (Fig. 2*D*). These data strongly indicate that Nur77 plays an important role in limiting the activation of CD4$^+$ T cells, which is pivotal for restricting the spontaneous development of T cell-mediated, organ-specific autoimmunity.

Along these lines, the disease course was also aggravated in Nur77^{KO} mice compared with WT controls in the active MOG$_{35–55}$–induced EAE model. Nur77^{KO} mice exhibited an earlier disease onset and a significantly aggravated mean clinical EAE score (Fig. 2*E*), accompanied by increased lesion burden, CNS infiltration of CD3$^+$ T cells, and enhanced demyelination (Fig. 2*F*). Assessment of MOG-specific CD4$^+$ T cells responses both in the periphery and the CNS at the peak of disease (day 15) revealed a significant increase in the numbers of IFN-γ– and IL-17A–producing MOG$_{35–55}$–specific T cells both in peripheral lymph nodes and within the CNS, whereas Treg frequencies remained unaffected (Fig. 2 *G* and *H*). Importantly, the increased production of proinflammatory cytokines by MOG$_{35–55}$–activated CD4$^+$ T cells was already visible before disease onset (i.e., on day 10), indicating that Nur77 limits T cell responses very early in the onset of T cell-mediated autoimmunity (Fig. 2*I*).

To address whether differences in T cell responses might be due to enhanced activation of APCs, we characterized splenic CD11c$^+$ DCs at 5 d after immunization. We found no differences between Nur77^{KO} and WT DCs regarding the expression of MHC-II, CD80, CD86, and CD40 (*SI Appendix*, Fig. S3*A*), as well as production of cytokines TNF-α, IL-12, and IL-6 (*SI Appendix*, Fig. S3*B*). These data strongly suggest that Nur77 deficiency in APCs does not substantially contribute to the observed increase in proinflammatory effector T cell responses during CNS autoimmunity.

To further confirm that Nur77 in T cells is important for the observed EAE phenotype, we performed adoptive transfer EAE experiments in which we either transferred CD4$^+$ T cells from MOG$_{35–55}$–immunized WT or Nur77^{KO} mice into WT recipients (Fig. 2*J*) or transferred WT CD4$^+$ T cells into WT or Nur77^{KO} recipients (Fig. 2*K*). Importantly, only the transfer of Nur77^{KO} T cells into WT recipients resulted in the development of significantly aggravated clinical symptoms compared with transfer of WT T cells. Of note, we did not observe any differences between Nur77^{KO} and Nur77^{WT} T cells before in vivo transfer with respect to exhaustion markers (e.g., CTLA-4, PD-1, BTLA, LAG-3) (21) and exhaustion-related cytokines (*SI Appendix*, Fig. S3*C*). In summary, Nur77 deficiency in T cells augments effector T cell responses and facilitates the development of T cell-mediated CNS autoimmunity in different animal models.

Nur77 Limits Cell Cycle Progression and Metabolic Activity of Activated CD4$^+$ T Cells. In light of the role of Nur77 in apoptosis of immature lymphocytes within the thymus, we next addressed whether augmented T cell responses in Nur77^{KO} mice might be linked to changes in T cell apoptosis (12, 13). Interestingly, we did not observe any differences in the proportion of apoptotic T cells either ex vivo after isolation from Nur77^{KO} and WT mice or at 48 h after in vitro stimulation with αCD3/αCD28 (Fig. 3*A* and *SI Appendix*, Fig. S4*A*). Moreover, in vivo we could not link Nur77 deficiency in 2D2 T cells to changes in T cell apoptosis either directly ex vivo or after short-term stimulation of MOG$_{35–55}$–reactive T cells (Fig. 3*B* and *SI Appendix*, Fig. S4*B*). However, Nur77^{KO} T cells displayed an increased ability to move through the cell cycle, as proliferating cell nuclear antigen (PCNA) was up-regulated significantly earlier in Nur77-deficient CD4$^+$ T cells on TCR stimulation (*SI Appendix*, Fig. S4*C*), which

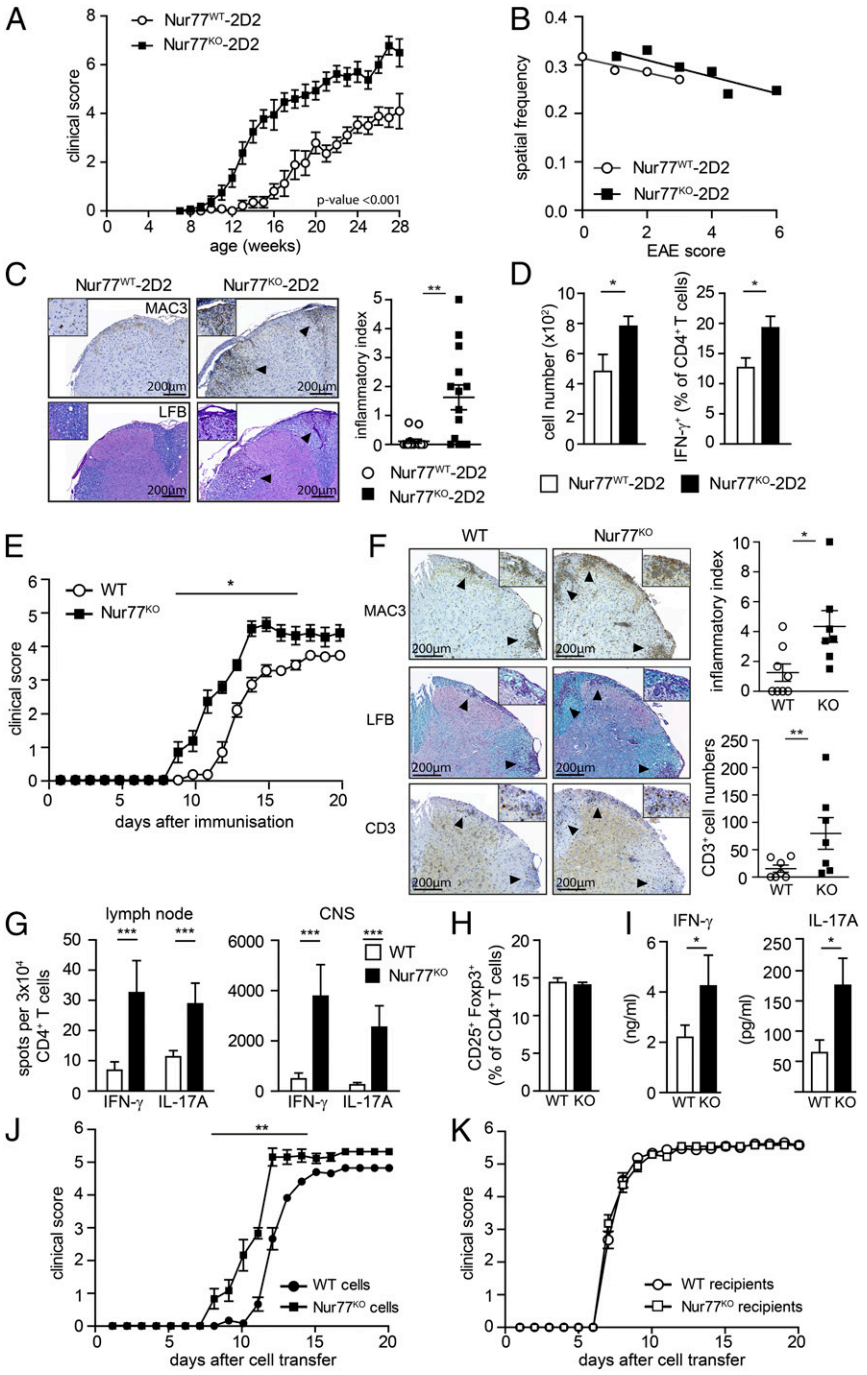

Fig. 2. Nur77 restricts T cell-mediated autoimmunity. (*A*) Clinical monitoring of Nur77^{WT}-2D2 ($n = 15$) and Nur77^{KO}-2D2 ($n = 16$) mice. Statistical analysis is described in *Methods*. (*B*) Spatial frequency was recorded in 15-wk-old Nur77^{WT}-2D2 and Nur77^{KO}-2D2 mice and is shown based on clinical score; $n = 4$–6/group. (*C*) Histological analysis was performed in 25-wk-old mice from *A* with regard to infiltration of myeloid cells (MAC3) and demyelination [luxol fast blue (LFB)]. (Scale bars: 200 μm.) Graph depicts mean inflammatory index; $n = 14$/group. (*D*) Cell numbers (*Left*) and IFN-γ-production (*Right*) of CNS infiltrating CD4$^+$ T cells in 15-wk-old mice from *A* were determined by flow cytometry; $n = 8$/group. (*E*) Active EAE was induced by $MOG_{35–55}$ immunization in WT and Nur77^{KO} mice. Mean clinical score of two pooled independent experiments is depicted; $n = 15$/group. (*F*) On day 13 of EAE, mice from *E* were histologically analyzed for infiltration of myeloid cells (MAC3), T cells (CD3), and demyelinated area (LFB). (Scale bars: 200 μm.) Graphs show the mean inflammatory index and number of CD3$^+$ T cells in the white matter; $n = 7$/group. (*G*) Numbers of IL-17A– and IFN-γ–producing CD4$^+$ T cells were determined on day 15 of EAE in lymph nodes and CNS by ELISpot analysis after ex vivo restimulation with $MOG_{35–55}$ for 24 h; $n = 10$/group. (*H*) On day 15 post-immunization, the frequency of Treg cells was determined in draining lymph nodes; $n = 6$/group. (*I*) Splenocytes were isolated from $MOG_{35–55}$–immunized mice on day 10 of EAE and then ex vivo stimulated with $MOG_{35–55}$. Cytokine secretion was determined by ELISA; $n = 6$/group. (*J* and *K*) Adoptive transfer EAE experiments were performed with either transfer of WT and Nur77^{KO}cells into WT recipients (*J*) or transfer of WT cells into WT and Nur77^{KO} recipients (*K*). Shown is the clinical score. Graphs depict mean ± SEM. Additional information on all EAEs is provided in *SI Appendix*, Table S6. Shown is one representative experiment out of at least two experiments. Statistical analysis was performed using Student's *t* test and two-way ANOVA with Bonferroni posttest (*E*, *I*, and *J*). $*P \leq 0.05$; $**P \leq 0.001$; $***P \leq 0.001$.

might have contributed to the observed enhanced spontaneous and antigen-induced proliferation of Nur77-deficient T cells.

As it is known that entry into cell division and cell cycle progression is closely regulated by metabolic pathways (22), we wondered whether Nur77 might modulate T cell metabolism to regulate T cell function. To this end, we compared the metabolic profiles of Nur77^{KO} T cells and their WT counterparts in terms of mitochondrial respiratory function and aerobic glycolysis on TCR-mediated stimulation. Interestingly, Nur77^{KO} T cells exhibited significantly enhanced basal and maximal respiration as well as enhanced glycolysis and glycolytic capacity (Fig. 3*C*), indicating that Nur77 deficiency in T cells provides a distinct metabolic advantage, facilitating the generation of the fuel and building blocks necessary for the proliferation and acquisition of effector functions.

We then performed time course experiments to evaluate when Nur77-mediated effects on T cell metabolism become visible, and found that Nur77-dependent effects on mitochondrial respiration and aerobic glycolysis could be observed as early as 24 h after αCD3 stimulation (Fig. 3*D* and *SI Appendix*, Fig. S4*D*). Of note, we observed that Nur77^{KO} T cells have an enhanced flexibility to switch between both key energy pathways compared with WT T cells. Pharmacologic inhibition of either mitochondrial respiration by rotenone or glycolysis by 2-deoxy-D-glucose (2-DG) alone had a significantly reduced inhibitory effect on the proliferation of Nur77^{KO} T cells compared with WT T cells (Fig. 3*E* and *SI Appendix*, Fig. S4*E*). This suggests that lack of Nur77 increases the capacity of T cells to optimize energy generation even under suboptimal conditions. Taken together, these data demonstrate that Nur77 restricts the metabolism of activated

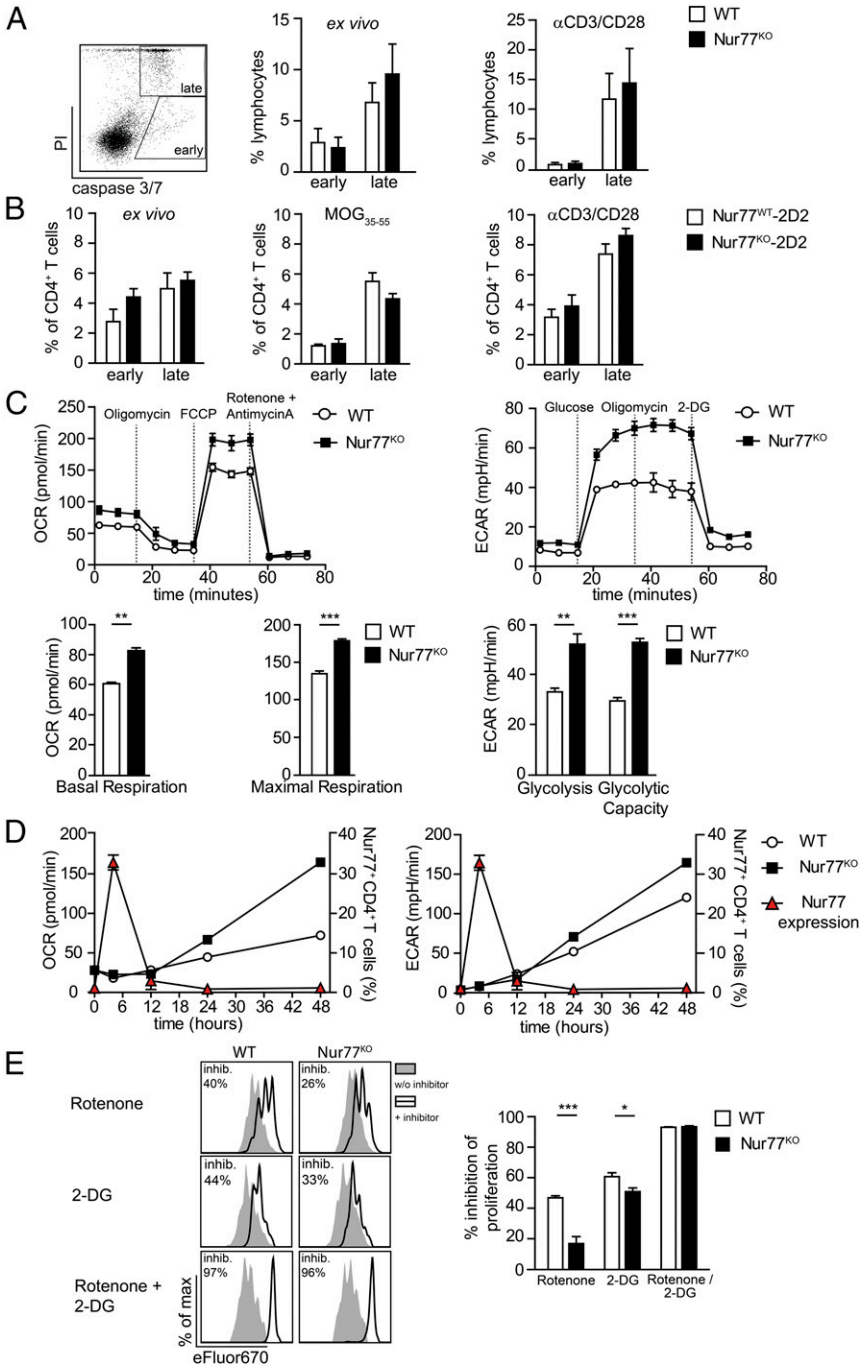

Fig. 3. Nur77 limits T cell responses by restriction of T cell metabolism and cell cycle progression. (*A* and *B*) Frequencies of early apoptotic (Caspase3/7$^+$, PI$^-$) and late apoptotic (Caspase3/7$^+$, PI$^+$) CD4$^+$ T cells were determined in spleens of WT or Nur77^{KO} mice (*A*) and in Nur77^{WT}-2D2 or Nur77^{KO}-2D2 mice (*B*), respectively. Frequency of early and late apoptotic T cells was assessed either ex vivo or after 72 h of stimulation with αCD3/αCD28 (*A* and *B*) or addition of MOG_{35-55} (*B*); $n = 5$ mice/group. (*C*) Oxygen consumption rate (OCR) and extracellular acidification rate (ECAR) by CD4$^+$ T cells were determined after 72 h of αCD3/αCD28 stimulation. Graphs depict mean basal and maximal respiration (*Left*) or mean glycolysis and glycolytic capacity (*Right*). (*D*) Basal respiration and glycolysis of activated WT and Nur77^{KO} CD4$^+$ T cells analyzed at the indicated time points. In parallel, Nur77 expression of stimulated WT CD4$^+$ T cells was determined. (*E*) CD4$^+$ T cells were stimulated with αCD3/αCD28 for 3 d. Rotenone (100 nM) and/or 2-deoxy-D-glucose (2-DG) (5 mM) were initially added during stimulation as indicated. T cell proliferation was assessed by flow cytometry, and the percentage of inhibition was calculated by (% proliferation [without inhibitor])/(% proliferation [± Rotenone ± 2-DG]). Graphs depict mean ± SEM. Shown is one representative experiment out of three experiments, unless stated otherwise. Statistical analysis was assessed with Student's *t* test. $*P \leq 0.05$; $**P \leq 0.001$; $***P \leq 0.001$.

T cells, which might contribute to the control of effector T cell responses.

Nur77 Regulates Metabolic Gene Expression in Activated T Cells. Given that Nur77 is a transcription factor, we next evaluated whether the observed metabolic changes might be linked to an altered transcriptional profile in Nur77^{KO} vs. WT CD4$^+$ T cells. We first performed quantitative RT-PCR arrays to examine the gene expression profiles of 168 genes associated with glucose and mitochondrial metabolism in naïve and activated T cells (Nur77^{KO} vs. WT). A Venn diagram analysis identified 87 of 94 differentially expressed metabolic genes as dependent on TCR stimulation, suggesting that TCR stimulation profoundly changes the metabolic transcription profile of T cells. Interestingly, almost one-half (10 of 21) of the Nur77-regulated metabolic genes were also dependent on TCR stimulation, pointing toward a key role of Nur77-dependent gene regulation in T cells during activation (Fig. 4*A*). Further analysis of gene expression levels showed that Nur77-deficient T cells exhibited a statistically significant difference in the expression of several electron transport genes, as well as genes involved in glucose metabolism, compared with WT T cells (*SI Appendix*, Fig. S5*A*). Differential gene expression was confirmed by independent quantitative RT-PCR analysis (*SI Appendix*, Fig. S5*B*). Notably, gene expression network analysis using Pearson correlation revealed a slight but widespread (87%) increase in expression of metabolic genes in Nur77-deficient T cells, including both electron transport genes (rectangles) and genes involved in glucose metabolism (circles) (Fig. 4*B*).

To corroborate the RT-PCR array data, unbiased RNA sequencing (RNA-Seq) was performed, comparing Nur77-deficient and Nur77-competent T cells. Again, Venn diagram analysis identified 11,487 of 11,638 differentially expressed genes and, importantly, almost all (3,344 of 3,725) Nur77-regulated genes as dependent on TCR stimulation (Fig. 4*C*). Furthermore, principal component analysis and hierarchical clustering revealed profound differences in the expression levels of numerous genes (including metabolic genes) in Nur77-deficient T cells compared with their WT counterparts (Fig. 4 *D* and *E* and *SI Appendix*, Table S1). Interestingly, gene regulatory network mapping based on motif enrichment in a coexpressed gene set via iRegulon (Fig. 4*B*) did not reveal enrichment of Nur77-binding sites in promoter regions of the investigated metabolic genes; however, we could identify five transcription factors (*Esrra*, *Esrrg*, *Esrrb*, *Nr2f1*, and *Nr0b1*; hexagons) that were predicted to regulate a majority of the investigated metabolic genes (102 of 168). This finding suggests that Nur77 may serve as master transcription factor regulating metabolic signatures in T cells via interaction with other transcription factors.

Nur77 Binds Genes Required for Key Metabolic Functions. We next aimed to identify direct transcriptional targets of Nur77 in $CD4^+$ T cells during activation using genome-wide chromatin immunoprecipitation (ChIP) with Nur77-specific antibodies, followed by sequencing (ChIP-seq). We identified Nur77 binding to several genes encoding for transcription factors known to regulate T cell metabolism following activation, including *Rps6ka*, *Mapk3*, *Rictor*, and *Notch2* (Fig. 5*A*). Indeed, expression of these transcription factors was significantly up-regulated in Nur77-deficient T cells, suggesting that Nur77 acts as a transcriptional repressor of these transcription factors (*SI Appendix*, Fig. S5*C*). Importantly, Nur77 also bound to *Esrra* (Fig. 5*A*), a gene encoding for the ERRα, which was already identified by our iRegulon analysis before (Fig. 4*B*). Our RNA-Seq analysis revealed that gene expression of ERRα target genes was significantly altered in Nur77-deficient cells compared with Nur77-competent T cells (*SI Appendix*, Table S2). A Gene Ontology (GO) database analysis further illustrated that ERRα target genes are linked to transcription regulation ($P = 2.6 \times 10^{-3}$) and mitochondrial-associated processes ($P = 4.6 \times 10^{-3}$), and approximately 30% of GO term-related ERRα target genes were significantly altered in Nur77-deficient T cells (*SI Appendix*, Table S3). In line with our ChIP-seq data, flow cytometric analysis revealed that ERRα protein expression was significantly upregulated in activated $Nur77^{KO}$ $CD4^+$ T cells compared to WT $CD4^+$ T cells (Fig. 5*B*). These findings are of particular interest in light of the ERRα-mediated control of T cell metabolism and CNS autoimmunity (4).

ERRα Inhibition Partially Reverses Nur77-Mediated Effects on T Cell Metabolism and T Cell-Mediated CNS Autoimmunity. Given the foregoing findings, we asked whether Nur77-mediated effects on T cells might be at least partially mediated via ERRα. We first performed RNA-Seq experiments of stimulated Nur77-competent and Nur77-deficient T cells in the presence or absence of XCT790 or Compound A (CompA), two pharmacologic ERRα inhibitors. Of note, pharmacologic ERRα inhibition equalized the expression levels of several ERRα target genes in Nur77-deficient T cells to WT levels (Fig. 5*C*). Furthermore, pharmacologic ERRα inhibition by XCT790 or CompA partially reversed the increase in proinflammatory cytokine production in $Nur77^{KO}$ T cells (Fig. 5*D* and *SI Appendix*, Fig. S5*D*), and increased mitochondrial respiration and glycolysis in $Nur77^{KO}$ T cells was reversed to WT levels by pharmacologic blockade of ERRα in vitro (Fig. 5*E* and *SI Appendix*, Fig. S5*E*).

Importantly, treatment of mice with the ERRα inhibitor XCT790 during active EAE reversed both the earlier disease onset and the aggravated mean clinical EAE score of Nur77-deficient mice, whereas the EAE disease course of WT mice was not significantly affected (Fig. 5*F*). At the peak of disease (day 13), mice were killed, and CNS-derived $CD4^+$ T cells were

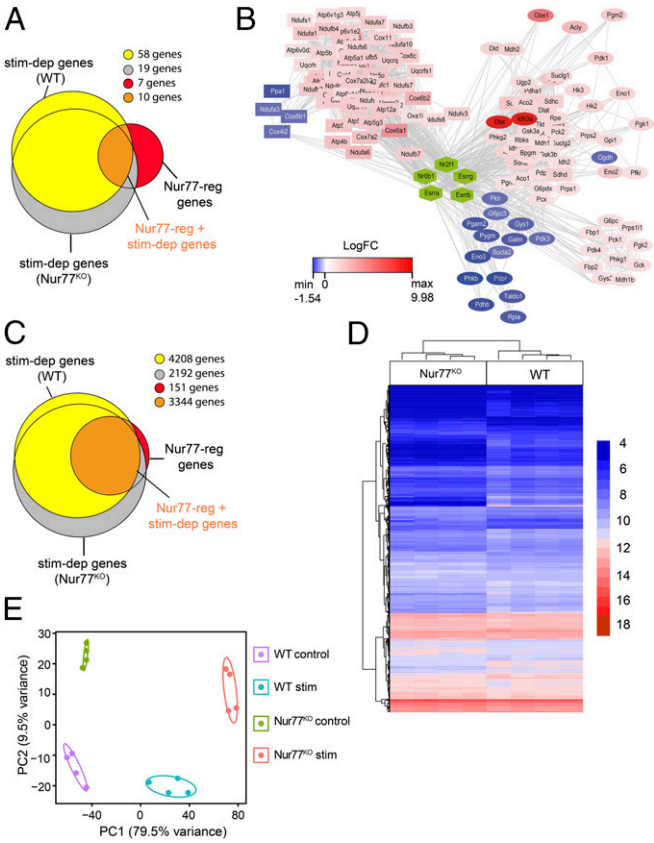

Fig. 4. Nur77 regulates genes required for metabolic functions. (*A* and *B*) Gene expression analysis of mitochondrial energy metabolism and glucose metabolism genes was performed with αCD3/αCD28-activated $Nur77^{KO}$ and WT $CD4^+$ T cells; $n = 6$ mice/group. (*A*) Venn diagram of all significant differential expressed genes (false discovery rate, <0.05). The orange color in the Venn diagram indicates the overlap between genes regulated by T cell stimulation (stim-dep genes) and genes regulated by Nur77 (Nur77-reg genes) (stim-dep WT genes, $n = 68$; stim-dep $Nur77^{KO}$ genes, $n = 78$; Nur77-reg genes, $n = 21$). (*B*) Functional gene expression network of stimulated $Nur77^{KO}$ vs. WT $CD4^+$ T cells (Pearson correlation coefficient ≥0.9), showing analysis of all investigated OXPHOS genes (rectangle) and glycolytic genes (circle), indicated as increasedly (red) or decreasedly expressed (blue). iRegulon-based analysis led to the identification of five transcription factors (hexagon) with enriched binding sites among network genes. (*C*–*E*) Unbiased RNA-Seq analysis was performed with αCD3/αCD28-activated $Nur77^{KO}$ and WT $CD4^+$ T cells; $n = 4$ mice/group. (*C*) Venn diagram of all significant differentially expressed genes (false discovery rate, <0.05). Orange indicates the overlap between genes regulated by T cell stimulation (stim-dep genes) and genes regulated by Nur77 (Nur77-reg genes) (stim-dep WT genes, $n = 8,357$; stim-dep $Nur77^{KO}$ genes, $n = 10,549$; Nur77-reg genes, $n = 3,725$). (*D*) Heatmap depicting the normalized and transformed read counts of all significant genes from the activated $Nur77^{KO}$ and WT $CD4^+$ T cells. (*E*) Principal component analysis of data from *D* including $Nur77^{KO}$ and WT $CD4^+$ T cells under control conditions (unstimulated).

analyzed. Pharmacologic ERRα inhibition reduced the numbers of IFN-γ– and IL-17A–producing $CD4^+$ T cells in the CNS in Nur77-deficient mice to WT levels, whereas the numbers in WT mice remained unaffected (Fig. 5*G*). Furthermore, pharmacologic ERRα inhibition in vivo reversed the increased metabolic activity of Nur77-deficient T cells, but not the Nur77-competent T cells, of lymph nodes derived from EAE animals, as illustrated by enhanced basal respiration and glycolysis (Fig. 5*H*).

Finally, shRNA-mediated knockdown of *Esrra* expression in stimulated murine Nur77-deficient, but not WT $CD4^+$, T cells reduced the elevated frequencies of the proinflammatory cytokine IFN-γ (Fig. 5*I* and *SI Appendix*, Fig. S5*F*). Furthermore, shRNA knockdown of *Esrra* lowered the increased metabolic gene expression of Nur77-deficient T cells (Fig. 5*J*). Taken together, these data

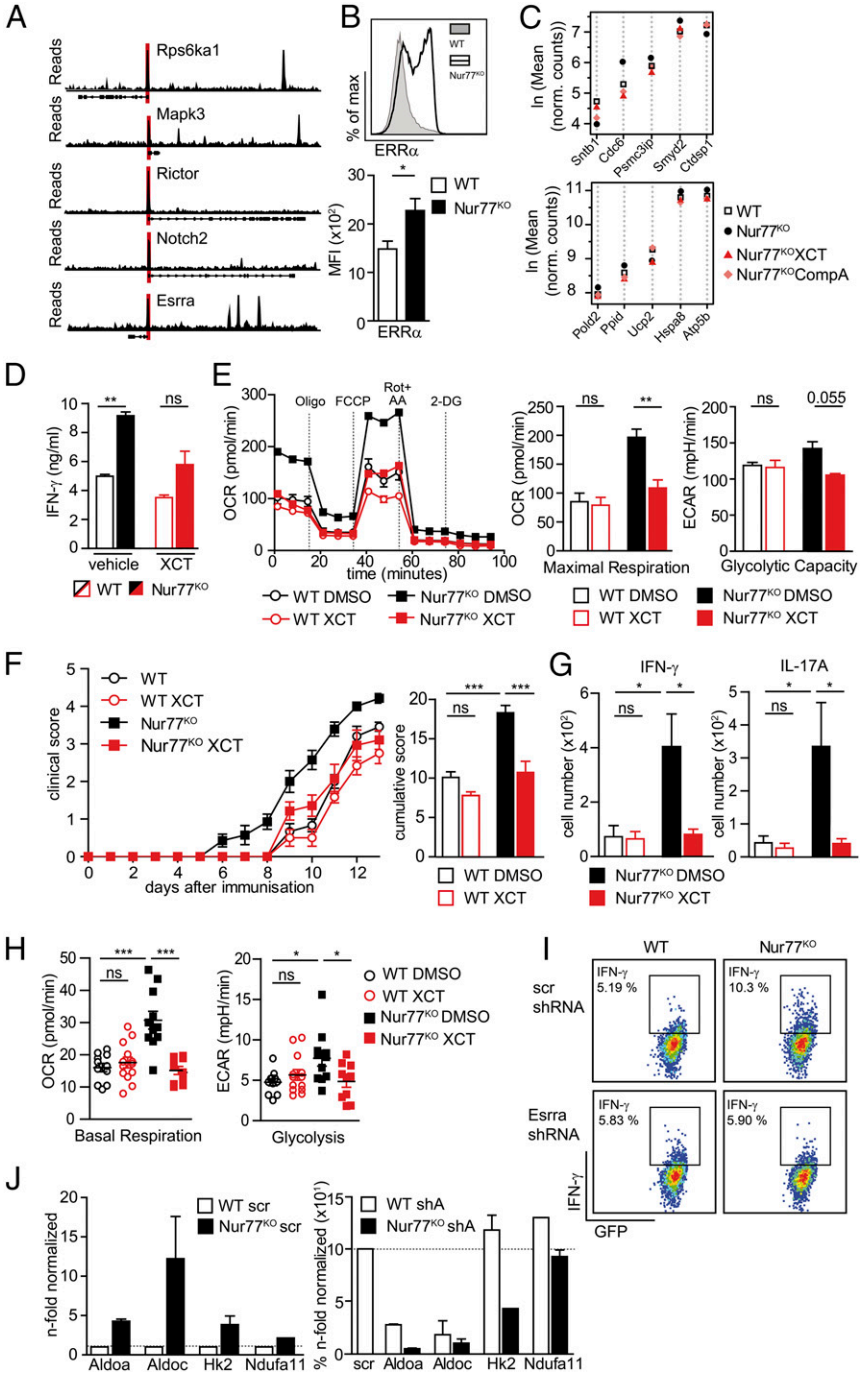

Fig. 5. ERRα inhibition partially reverses Nur77-mediated effects on T cell metabolism and T cell-mediated CNS autoimmunity. (*A*) ChIP-seq analysis of WT CD4$^+$ T cells activated with αCD3/αCD28 for 4 h. Nur77 binds to target genes encoding for transcription factors that regulate T cell metabolism. The red line displays a narrow peak region from peak calling with MACS2 ($q < 0.05$; $n = 6$/group). (*B*) ERRα expression by WT and Nur77^{KO} CD4$^+$ T cells after 72 h of αCD3/αCD28 stimulation. Shown is a representative histogram; the graph depicts the mean fluorescence intensity (MFI) of ERRα expression; $n = 4$/group. (*C*) WT or Nur77^{KO} CD4$^+$ T cells were activated with αCD3/αCD28 for 12 h in the presence of ERRα inhibitors XCT790 (XCT; 10 μg/mL) or Compound A (CompA; 10 μg/mL) before T cells were subjected to RNA-Seq. Both plots depict the natural logarithm of the mean of normalized read counts from ERRα target genes; $n = 4$ mice/group. (*D*) WT or Nur77^{KO} CD4$^+$ T cells were αCD3/αCD28-activated and treated with 2.5 μg/mL XCT. After 72 h, the mean cytokine production was determined by ELISA. (*E*) Maximal respiration and glycolytic capacity of αCD3/αCD28-stimulated WT and Nur77^{KO} CD4$^+$ T cells was determined on day 3 of αCD3/αCD28 stimulation in the presence or absence of XCT (2.5 μg/mL). Shown is a representative run. Bar graphs depict OCR and ECAR; $n = 3$ mice/group. (*F*) MOG_{35-55} EAE was induced in WT or Nur77^{KO} mice. In parallel, 5 mg/kg body weight XCT or vehicle only (DMSO) were administered daily by oral gavage. Shown is the mean clinical score; the graph depicts the mean ± SEM cumulative clinical score; $n = 7$/group. (*G*) On day 13 postimmunization, numbers of CNS-specific Th1 and Th17 cells were determined by flow cytometry; $n = 6$/group. (*H*) On day 10 of EAE, T cells were isolated from draining lymph nodes, and basal respiration as well as glycolysis was determined ex vivo; $n = 10$–13/group. (*I* and *J*) Nur77^{KO} or WT CD4$^+$ T cells were lentivirally transfected with control-shRNA (scr) or *Esrra*-shRNA (shA) and subsequently stimulated with αCD3/αCD28 for 72 h. (*I*) Then IFN-γ production was assessed by flow cytometry; representative dot plots are shown. (*J*) Alternatively, qRT-PCR analysis of metabolic genes was performed. Graphs display mean ± SEM. Statistical analysis was performed using Student's *t* test and two-way ANOVA with Bonferroni posttest (*F*–*H*). Shown is one representative experiment out of three experiments, unless stated otherwise. *$P \leq 0.05$; **$P \leq 0.001$; ***$P \leq 0.001$. Oligo, oligomycin; Rot, rotenone; AA, antimycin A; 2-DG, 2-deoxy-D-glucose.

support the idea that Nur77-mediated control of T cell metabolism involves the integration of downstream factors including ERRα, which then regulate metabolic programming in T cells.

Nur77 in T Cells Limits T Cell-Mediated Inflammatory Diseases. Finally, we wondered whether Nur77 might also restrict T cell responses in the context of other T cell-mediated inflammatory diseases. We first assessed T cell responses in a model of hapten-induced (DNFB) allergic contact dermatitis comparing Nur77^{KO} mice and WT mice. Nur77^{KO} mice exhibited significantly enhanced ear swelling (Fig. 6*A*) and subcutaneous edema compared with WT mice (Fig. 6 *A* and *B*). This was accompanied by increased numbers of CD4$^+$ and CD8$^+$ T cells in the draining lymph nodes (Fig. 6*C*), of which an increased proportion produced IFN-γ (Fig. 6*C*) and expressed enhanced levels of the activation marker CD69, whereas Treg frequencies remained unaffected (Fig. 6*D* and *SI Appendix*, Fig. S6*A*).

In addition, in a model of collagen-induced arthritis, we observed that CD4$^+$ and CD8$^+$ T cells isolated from Nur77^{KO} mice produced significantly greater amounts of cytokines and showed enhanced activation on restimulation ex vivo (Fig. 6*E*), although we did not find a change in overall disease severity (Fig. 6*F*). This is most likely due to the relevance of non-T cells, such as macrophages, fibroblasts and osteoclasts, in destructive joint inflammation (23, 24). Of note, in this model, Treg frequencies were not altered in Nur77^{KO} mice (*SI Appendix*, Fig. S6*B*).

In summary, these data provide evidence that Nur77 plays a central role in the control of T cell responses in the context of different T cell-mediated inflammatory diseases, highlighting the

overall relevance of this key modulator of T cell metabolism for the control of T cell-mediated inflammatory diseases.

Discussion

Here we have identified Nur77 as key modulator of T cell function restricting activation, cell cycle progression, and proliferation, which limits aberrant effector T cell responses and impedes the development of T cell-mediated inflammatory diseases. Mechanistically, Nur77 controls a complex metabolic network partly via interaction with the transcription factor ERRα, which results in alteration of the T cell energy metabolism, impacting the generation of the fuel and building blocks essential for rapid cell activation and expansion.

Nur77 has been implicated in apoptosis during negative selection in thymic T cell development (12, 13). Given the spontaneous accumulation of T cells in Nur77-deficient mice, we assumed that lack of Nur77 might alter T cell apoptosis, thereby promoting T cell expansion. However, we could not link Nur77 deficiency to changes in T cell apoptosis neither in vitro or ex vivo nor on short-term restimulation. These results are in line with other studies that also found no impact of Nur77 on the apoptosis of mature T cells (11, 25). Instead, we observed that Nur77 contributes to the modulation of cell cycle progression, as indicated by accelerated up-regulation of PCNA in activated Nur77-deficient T cells (*SI Appendix*, Fig. S4*C*). Along this line, Nur77 deficiency resulted in enhanced homeostatic T cell proliferation in vivo, paralleled by spontaneous T cell activation and memory formation.

These findings suggest that the absence of Nur77 lowers the threshold for T cell activation and facilitates T cell activation even in the absence of an exogenous stimulus (26, 27). Nur77 protein is induced within hours after TCR stimulation (11), and we further found that its expression does not depend on additional costimulatory signals or polarizing cytokines, indicating that its expression is linked to TCR activation itself. This suggests that Nur77 is implicated in the control of T cell activation per se rather than being limited to distinct T cell subpopulations. Importantly, its expression in T cells is transient, suggesting that it exerts its function early during T cell activation (28).

As key checkpoints of cell cycle progression and proliferation are known to be controlled by metabolic pathways (22), we investigated whether Nur77 might have an impact on T cell metabolism. Indeed, Nur77-deficiency conferred a metabolic advantage, with Nur77^{KO} T cells showing enhanced aerobic glycolysis and mitochondrial respiration. An influence of Nur77 on metabolic pathways has been previously documented in skeletal muscle cells and hepatocytes, cells known for their high metabolic activity (29, 30); however, its role in the modulation of immune cell metabolism has not been addressed so far.

In recent years, accumulating evidence shows that on activation, lymphocytes undergo a dramatic metabolic reprogramming to meet their increased energy demands. Several metabolic pathways have been linked to T cell function; for example, glycolysis is pivotal for effector functions of CD4$^+$ T cells (31), whereas long-lived memory T cells depend strongly on oxidative phosphorylation (OXPHOS) to meet their energy demands and enable functionality (5).

Therefore, it is conceivable that increased metabolic activity and optimized fuel consumption in the absence of Nur77 might promote proinflammatory T cell responses and thus facilitate the development of T cell-mediated autoimmunity. Interestingly, other factors influencing T cell metabolism also have strong impacts on the development of autoimmunity. One example is HIF-1α, which promotes metabolic reprogramming of T cells to maintain proliferation and effector function at hypoxic inflammatory sites (32). A lack of HIF-1α in mice was found to result in diminished Th17 but enhanced Treg cell differentiation and to protect against CNS inflammation (33). We now contribute to this concept by providing evidence that Nur77 also controls the development of aberrant T cell responses and autoimmunity via metabolic programming of T cells.

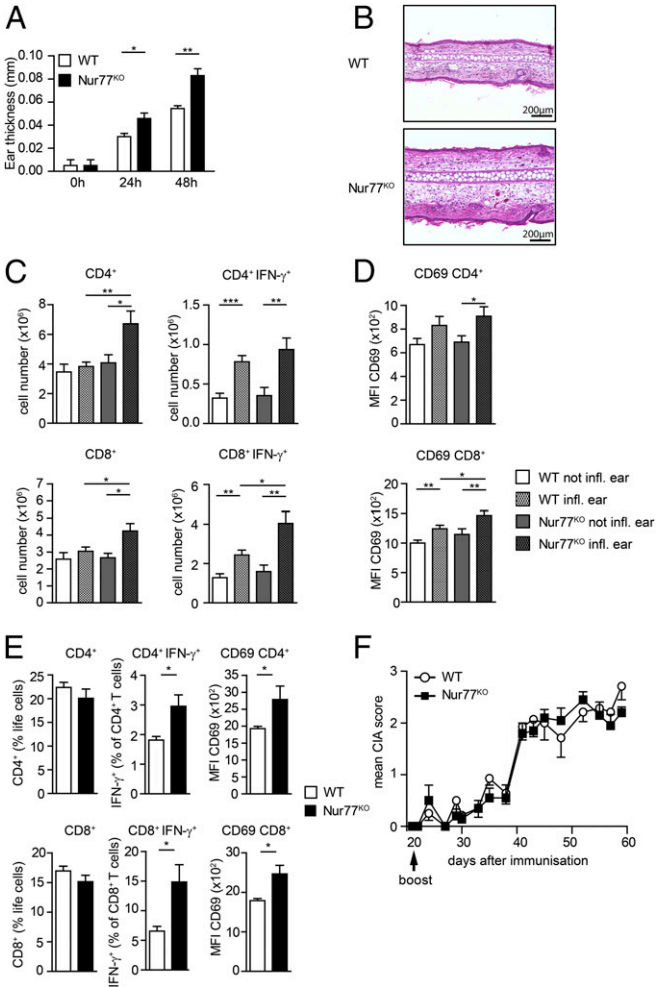

Fig. 6. Nur77 restricts T cell responses in contact dermatitis and autoimmune arthritis. (*A–D*) Allergic contact dermatitis (ACD) was induced in C57BL/6J or Nur77^{KO} mice. (*A*) Relative ear thickness of mice was determined; n = 7–9/group. (*B*) On day 2 of ACD, ear tissue was stained with hematoxylin and eosin; n = 7 mice/group. (Scale bars: 200 μm.) (*C*) Numbers of CD4$^+$ and CD8$^+$ T cells (*Left*) and IFN-γ$^+$ CD4$^+$ and CD8$^+$ T cells (*Right*) were determined in auricular and axillar lymph nodes by flow cytometry; n = 6/group. (*D*) In addition, expression of CD69 on T cells was determined by flow cytometry; the mean fluorescence intensity (MFI) is depicted. Shown is one representative out of two experiments. (*E* and *F*) Collagen-induced arthritis (CIA) was induced in WT and Nur77^{KO} mice by Collagen type II immunization. (*E*, *Left*) On day 59 of CIA, cell numbers of CD4$^+$ and CD8$^+$ T cells and intracellular cytokine production (IFN-γ) of both cell types were determined in inguinal and popliteal lymph nodes by flow cytometry. (*E*, *Right*) Mean MFI of CD69 in CD4$^+$ and CD8$^+$ T cells; n = 6/group. (*F*) Clinical evaluation of CIA induced in WT and Nur77^{KO} (n = 8–10/group) (*SI Appendix*, Table S6). Data were generated in one experiment. Infl., inflamed. Data are depicted as mean ± SEM. *$P \leq 0.05$; **$P \leq 0.001$; ***$P \leq 0.001$.

Several aspects of Nur77-mediated modulation of T cell metabolism and autoimmunity are noteworthy. First, Nur77 activation and Nur77-dependent effects occur very early in TCR-mediated T cell activation and are not limited to specific T effector differentiation processes. Second, memory T cells exhibit a less pronounced induction of Nur77 expression on TCR stimulation, which may limit Nur77-mediated repression of T cell metabolism and thereby contribute to the known metabolic advantage of memory T cells (*SI Appendix*, Fig. S6*C*) (5). Third, given that metabolic and functional alterations of T cells could be observed already in cells derived from young healthy mice, it can be concluded that Nur77-dependent alterations precede the observed increase in autoimmunity and are not a consequence thereof.

Mechanistically, analysis of the metabolic transcriptional network via RNA-Seq and real-time RT-PCR revealed that Nur77 modulates expression of numerous genes involved in metabolic pathways, although the impact on individual gene expression levels is rather modest. However, analysis of transcription factor binding sites of the investigated genes did not reveal an enrichment of Nur77-binding sites, suggesting that Nur77 does not directly alter transcription of the investigated genes. Instead, our network analysis suggests that Nur77 itself might regulate several metabolically relevant transcription factors, such as *Nr2f1*, *Nr0b1*, *Esrra*, *Esrrb*, and *Essrg*. Indeed, other transcription factors, including ERRα, mTOR, and HIF-1α, have been identified as metabolic regulators in T cells that exert their function either alone or in concert with other factors (4, 9, 32). Along this line, our ChIP sequencing analysis revealed direct binding of Nur77 protein to the *Esrra* promoter, and we found evidence of a functional interaction of Nur77 with the *Esrra* promoter in a luciferase reporter assay (*SI Appendix*, Fig. S6*D*).

Furthermore, flow cytometric analysis showed elevated ERRα protein expression in $Nur77^{KO}$ T cells, and pharmacologic inhibition of ERRα abrogated enhanced proinflammatory cytokine production, as well as the metabolic activity of activated $Nur77^{KO}$ $CD4^+$ T cells, but not WT T cells, in vitro. Accordingly, ERRα inhibition in vivo reversed enhanced disease activity and proinflammatory T cell infiltration into the CNS of $Nur77^{KO}$ mice during active EAE. Finally, lentiviral knockdown of ERRα reversed both proinflammatory cytokine production and enhanced gene expression of metabolic genes in Nur77-deficient T cells. Taken together, these results indicate that Nur77 affects T cell metabolism and thus proinflammatory T cell function at least in part via modulation of ERRα. In support of this concept, it has been reported that ERRα broadly affects metabolic gene expression and glucose metabolism of effector T cells, and that pharmacologic inhibition and deficiency of ERRα restricts T cell responses in vivo and ameliorates autoimmunity (4).

So far, Nur77 has not been identified as a transcriptional regulator of T cell metabolism and T cell-mediated autoimmunity. Using different animal models, including a spontaneous model of CNS autoimmunity, we have found evidence that Nur77 in T cells mediates enhanced CNS autoimmunity. Interestingly, Nur77 in DCs and macrophages seems to be dispensable for the observed phenotype, at least in our hands, as lack of Nur77 in DCs did not alter their antigen-presentation capacity and proinflammatory DC response during EAE (*SI Appendix*, Fig. S6*E*). Furthermore, there were no changes in the expression levels of costimulatory molecules in Nur77-deficient macrophages, except in MHC-II (*SI Appendix*, Fig. S6*F*). This finding was somewhat unexpected, given that Nur77 deficiency in macrophages has been linked to increased inflammatory activity in a model of atherosclerosis and EAE (25, 34).

Interestingly, it was recently shown that Nur77 deficiency in microglial cells promotes CNS inflammation during active EAE (35). Consequently, we characterized microglial responses in Nur77-deficient mice during EAE; however, we did not observe any alterations when assessing microglia cell counts or CD40 and MHC-II expression (data not shown). Furthermore, our adoptive transfer EAE experiments show that Nur77-deficiency in transferred T cells, but not in recipient mice, resulted in enhanced disease severity, providing further evidence that at least in the animal models used in our study, Nur77 seems to play no major role in CNS-resident cells in the context of CNS autoimmunity.

Double-transgenic $Nur77^{KO}$-2D2 mice spontaneously developed CNS autoimmunity at a higher frequency than $Nur77^{WT}$-2D2 mice, suggesting that Nur77 in T cells sets a threshold for the development of autoimmunity in susceptible mice, which further argues for a role of Nur77 during early control of T cell dysfunction. Along this line, we observed an increased proportion of cytokine-producing T cells when Nur77-deficient T cells were cultured in an APC-free system. Interestingly, despite the influence of Nur77 on distinct effector T cell subsets, such as Th1 and Th17 cells, we found no influence of Nur77 on Treg polarization in vitro or on Treg frequencies in healthy mice as well as in different animal models of T cell-mediated autoimmunity (Fig. 2*H* and *SI Appendix*, Fig. S6 *A*, *B*, *G*, and *H*). Furthermore, we did not observe an influence on Treg metabolism (*SI Appendix*, Fig. S6*I*). This finding was somewhat unexpected, as ablation of all three receptors of the NR4A family results in the development of systemic immunopathology due to functional alteration of Tregs, and given that Nur77 in Tregs has been shown to curtail Treg differentiation (36, 37). In this regard, we did not observe an altered sensitivity of effector T cells from $Nur77^{KO}$ mice or their WT counterparts toward the suppressive capacity of Tregs (*SI Appendix*, Fig. S6*J*).

Importantly, we found that Nur77 plays a general role in restricting proinflammatory T cell responses in various inflammatory diseases (i.e., CNS autoimmunity, allergic contact dermatitis and collagen-induced arthritis), underscoring the relevance of this pathway for cell-intrinsic modulation of the T cell activation threshold in vivo. This might have broad implications for the development of future treatment approaches in T cell-mediated inflammation and autoimmunity. In light of the potential relevance of Nur77 in CNS autoimmunity, we addressed Nur77 expression both in peripheral immune cells and within CNS inflammatory lesions in patients with MS. Interestingly, within the CNS, no Nur77 expression was observed within inflammatory lesions (data not shown), further highlighting the fact that Nur77 is rapidly but transiently expressed in human T cells on TCR triggering. Along this line, T cells directly isolated from the inflamed CNS of mice did not express Nur77 protein, but this expression could be rapidly induced on TCR stimulation (*SI Appendix*, Fig. S6*K*).

Regarding human T cell-mediated autoimmune diseases, genetic variants of Nur77 (SNPs) have been described for ulcerative colitis and Crohn`s disease as a result of large genome-wide association studies (GWAS), and these SNPs have been associated with an increased risk of disease (38). In contrast, no significant association between Nur77 and MS can be derived from publicly available GWAS data. However, it should be kept in mind that most genetic effects of complex diseases are indirect and act through (so-called) expression quantitative trait loci (QTLs), that is, through effects on downstream expression in the target tissue (here T cells). Furthermore, Nur77 might be implicated in the pathogenesis of autoimmunity in the absence of genetic variations, that is, via altered expression levels due to either decreased expression of transcriptional activators or increased expression of transcriptional repressors. In addition, functional alterations of Nur77, such as phosphorylation (39), might influence autoimmunity in the absence of genetic alterations within the *NR4A1* gene.

In summary, we have identified Nur77 as a regulator of T cell immunometabolism that elevates the threshold for T cell activation and serves as T cell-intrinsic brake for the development of aberrant T cell-mediated inflammation and autoimmunity. Thus, identification of receptor-specific pharmacologic agonists might prove to be a viable approach for treatment of T cell-mediated autoimmune diseases.

Methods

Mice and Cells. Nur77-deficient mice ($Nur77^{KO}$) (17) were purchased from Jackson Laboratories. The $Nur77^{KO}$ mice were crossed to OTII and 2D2 mice to generate $Nur77^{KO}$-OTII and $Nur77^{KO}$-2D2 mice, respectively. All strains—C57BL/6J, OTII, 2D2, $Nur77^{KO}$, $Nur77^{KO}$-OTII, $Nur77^{KO}$-2D2, and $Rag1^{KO}$ mice—were maintained under specific pathogen-free conditions in the central animal facility at the University of Münster in accordance with German guidelines for animal care. Unless stated otherwise, mice were used in the experiments at age 6–20 wk. Mice were excluded from the animal experiments as necessary according to the guidelines of the Animal Ethics Committee. All animal studies were performed without randomization but with blinding to the group allocation during the experiment. All experiments were performed in accordance with the guidelines of the Animal Experimental Ethics Committee and under approval by the local authorities of North Rhine-Westphalia, Germany. Media, T cell isolation and stimulation, and surface and intracellular staining are described in detail in *SI Appendix, Materials and Methods*.

EAE. Active and adoptive transfer EAE was performed with age- and sex-matched C57BL/6 and Nur77^{KO} mice. Spontaneous EAE disease incidence and severity were determined in 2D2 and Nur77^{KO}-2D2 mice. Details are provided in *SI Appendix, Materials and Methods*.

Metabolic Assays. CD4$^+$ T cells were stimulated with αCD3 and αCD28 (both 4 μg/mL plate-bound) for the indicated times. The oxygen consumption rate (OCR) was evaluated under basal conditions and in response to 1 μM oligomycin, 0.6 μM FCCP, 100 nM rotenone, plus 1 μM antimycin A (all from Sigma-Aldrich). The extracellular acidification rate (ECAR) was measured under basal conditions and in response to 100 mM glucose, 1 μM oligomycin, and 5 mM 2-DG (all from Sigma-Aldrich). Activated T cells were cultured in XF-medium (XF Base Medium Minimal DMEM; Agilent Technologies) containing 10 mM glucose, 2 mM L-glutamine, and 1 mM sodium pyruvate (all from Sigma-Aldrich). OCR and ECAR were determined using a Seahorse XFp or XFe96 Extracellular Flux Analyzer (Agilent), and assays were analyzed with Wave Desktop software (Agilent), as described in *SI Appendix, Materials and Methods*.

RT^2-PCR-Profiler PCR Array. CD4$^+$ T cells were isolated from C57BL/6 and Nur77^{KO} mice and stimulated with αCD3 and αCD28 for 12 h. RNA was isolated using the Qiagen RNeasy Mini Kit. The expression levels of glycolytic genes and genes involved in mitochondrial respiration were determined using RT^2 Profiler RCR Arrays (Qiagen), as described in *SI Appendix, Materials and Methods*.

RNA-Seq. CD4$^+$ T cells were isolated from C57BL/6 and Nur77^{KO} mice and then stimulated with αCD3 and αCD28 for 12 h with or without ERRα inhibitor XCT790 or Compound A. RNA was isolated using the Qiagen RNeasy Mini Kit. Samples with an RNA integrity number value >7 were selected for subsequent NGS library preparation, followed by sequencing with the NextSeq 500 system (Illumina). The analysis is described in detail in *SI Appendix, Materials and Methods*.

ChIP-Seq and Bioinformatics. CD4$^+$ T cells were isolated from C57BL/6 mice and subsequently stimulated with αCD3 and αCD28 for 4 h in vitro. Following cross-linking and sonication of genomic fragments, immunoprecipitation was performed with 3 μg of αNur77 (clone 12.14; eBioscience) and the corresponding polyclonal IgG control antibody (clone 12.14; eBioscience). Afterward, library preparation was performed using the NEBNext DNA Ultra II Kit (New England BioLabs), followed by sequencing with the Illumina NextSeq 500 system. Details are provided in *SI Appendix, Materials and Methods*.

Study Subjects. Blood sampling of healthy donors was approved by the local Ethics Committee (Ethikkommission der Ärztekammer Westfalen Lippe; 2016–053-f-S), and all subjects provided signed informed consent. Sample storage and subsequent analysis was performed after pseudonymization.

Statistical Analysis. All results are presented as mean ± SEM. Sample sizes were not chosen to ensure adequate power, to determine a predetermined effect size. GraphPad Prism software and R version 3.2.5 were used to perform statistical analysis. Student's *t* test was used for normally distributed data, and the Mann–Whitney U test was used for nonnormally distributed data. Fisher's exact test was used to compare categorical data between groups. The log-rank test was used to compare groups regarding time-to-event endpoints. Adoptive transfer EAE (Fig. 2 *J* and *K*) and active EAE (Fig. 2*E*) experiments were statistically analyzed using two-way ANOVA with Bonferroni's posttest. More information is provided in *SI Appendix, Materials and Methods*.

ACKNOWLEDGMENTS. We thank Annika Engbers, Andrea Pabst, and Claudia Kemming for technical support. This study was supported by Innovative Medical Research (Medical Faculty, University of Muenster) Grant I-HU121212 (to S.H. and L.K.), as well as German Research Foundation Grants CRC 128 A8 (to L.K.) and CRC 128 Z2 (to H.W. and T.K.). M.B. is a member of the Excellence Cluster ImmunoSensation.

1. Gizinski AM, Fox DA (2014) T cell subsets and their role in the pathogenesis of rheumatic disease. *Curr Opin Rheumatol* 26:204–210.
2. Hemmer B, Kerschensteiner M, Korn T (2015) Role of the innate and adaptive immune responses in the course of multiple sclerosis. *Lancet Neurol* 14:406–419.
3. Rathmell JC, Vander Heiden MG, Harris MH, Frauwirth KA, Thompson CB (2000) In the absence of extrinsic signals, nutrient utilization by lymphocytes is insufficient to maintain either cell size or viability. *Mol Cell* 6:683–692.
4. Michalek RD, et al. (2011) Estrogen-related receptor-α is a metabolic regulator of effector T-cell activation and differentiation. *Proc Natl Acad Sci USA* 108:18348–18353.
5. van der Windt GJW, et al. (2013) CD8 memory T cells have a bioenergetic advantage that underlies their rapid recall ability. *Proc Natl Acad Sci USA* 110:14336–14341.
6. Gerriets VA, et al. (2015) Metabolic programming and PDHK1 control CD4$^+$ T cell subsets and inflammation. *J Clin Invest* 125:194–207.
7. Mockler MB, Conroy MJ, Lysaght J (2014) Targeting T cell immunometabolism for cancer immunotherapy; understanding the impact of the tumor microenvironment. *Front Oncol* 4:107.
8. Freitag J, Berod L, Kamradt T, Sparwasser T (2016) Immunometabolism and autoimmunity. *Immunol Cell Biol* 94:925–934.
9. Liu Y, Zhang DT, Liu XG (2015) mTOR signaling in T cell immunity and autoimmunity. *Int Rev Immunol* 34:50–66.
10. Pearen MA, Muscat GE (2010) Minireview. Nuclear hormone receptor 4A signaling: Implications for metabolic disease. *Mol Endocrinol* 24:1891–1903.
11. Cunningham NR, et al. (2006) Immature CD4$^+$CD8$^+$ thymocytes and mature T cells regulate Nur77 distinctly in response to TCR stimulation. *J Immunol* 177:6660–6666.
12. Liu Z-G, Smith SW, McLaughlin KA, Schwartz LM, Osborne BA (1994) Apoptotic signals delivered through the T-cell receptor of a T-cell hybrid require the immediate-early gene nur77. *Nature* 367:281–284.
13. Calnan BJ, Szychowski S, Chan FK, Cado D, Winoto A (1995) A role for the orphan steroid receptor Nur77 in apoptosis accompanying antigen-induced negative selection. *Immunity* 3:273–282.
14. Ohashi PS (2003) Negative selection and autoimmunity. *Curr Opin Immunol* 15:668–676.
15. Li X-M, et al. (2015) Nur77 deficiency leads to systemic inflammation in elderly mice. *J Inflamm (Lond)* 12:40.
16. Guo Z, et al. (2010) IL-7, but not thymic stromal lymphopoietin (TSLP), during priming enhances the generation of memory CD4+ T cells. *Immunol Lett* 128:116–123.
17. Lee SL, et al. (1995) Unimpaired thymic and peripheral T cell death in mice lacking the nuclear receptor NGFI-B (Nur77). *Science* 269:532–535.
18. Bettelli E, et al. (2003) Myelin oligodendrocyte glycoprotein-specific T cell receptor transgenic mice develop spontaneous autoimmune optic neuritis. *J Exp Med* 197:1073–1081.
19. Miller PG, Bonn MB, Franklin CL, Ericsson AC, McKarns SC (2015) TNFR2 deficiency acts in concert with gut microbiota to precipitate spontaneous sex-biased central nervous system demyelinating autoimmune disease. *J Immunol* 195:4668–4684.
20. Schulze-Topphoff U, et al. (2013) Tob1 plays a critical role in the activation of encephalitogenic T cells in CNS autoimmunity. *J Exp Med* 210:1301–1309.
21. Crawford A, et al. (2014) Molecular and transcriptional basis of CD4$^+$ T cell dysfunction during chronic infection. *Immunity* 40:289–302.
22. Lee IH, Finkel T (2013) Metabolic regulation of the cell cycle. *Curr Opin Cell Biol* 25:724–729.
23. Papathanassiu AE, et al. (2017) BCAT1 controls metabolic reprogramming in activated human macrophages and is associated with inflammatory diseases. *Nat Commun* 8:16040.
24. Schett G, Stuhlmüller BG, Burmester G-R (2007) Cells of the synovium in rheumatoid arthritis: Osteoclasts. *Arthritis Res Ther* 9:203.
25. Shaked I, et al. (2015) Transcription factor Nr4a1 couples sympathetic and inflammatory cues in CNS-recruited macrophages to limit neuroinflammation. *Nat Immunol* 16:1228–1234.
26. Dunn SE, et al. (2010) Peroxisome proliferator-activated receptor delta limits the expansion of pathogenic Th cells during central nervous system autoimmunity. *J Exp Med* 207:1599–1608.
27. Klotz L, et al. (2009) The nuclear receptor PPAR gamma selectively inhibits Th17 differentiation in a T cell-intrinsic fashion and suppresses CNS autoimmunity. *J Exp Med* 206:2079–2089, and erratum (2009) 206:3159.
28. Ashouri JF, Weiss A (2017) Endogenous Nur77 is a specific indicator of antigen receptor signaling in human T and B cells. *J Immunol* 198:657–668.
29. Chao LC, et al. (2012) Skeletal muscle Nur77 expression enhances oxidative metabolism and substrate utilization. *J Lipid Res* 53:2610–2619.
30. Pei L, et al. (2006) NR4A orphan nuclear receptors are transcriptional regulators of hepatic glucose metabolism. *Nat Med* 12:1048–1055.
31. Chang CH, et al. (2013) Posttranscriptional control of T cell effector function by aerobic glycolysis. *Cell* 153:1239–1251.
32. Nakamura H, et al. (2005) TCR engagement increases hypoxia-inducible factor-1 alpha protein synthesis via rapamycin-sensitive pathway under hypoxic conditions in human peripheral T cells. *J Immunol* 174:7592–7599.
33. Shi LZ, et al. (2011) HIF1alpha-dependent glycolytic pathway orchestrates a metabolic checkpoint for the differentiation of TH17 and Treg cells. *J Exp Med* 208:1367–1376.
34. Hanna RN, et al. (2012) NR4A1 (Nur77) deletion polarizes macrophages toward an inflammatory phenotype and increases atherosclerosis. *Circ Res* 110:416–427.
35. Rothe T, et al. (2017) The nuclear receptor Nr4a1 acts as a microglia rheostat and serves as a therapeutic target in autoimmune-driven central nervous system inflammation. *J Immunol* 198:3878–3885.
36. Sekiya T, et al. (2013) Nr4a receptors are essential for thymic regulatory T cell development and immune homeostasis. *Nat Immunol* 14:230–237.
37. Fassett MS, Jiang W, D'Alise AM, Mathis D, Benoist C (2012) Nuclear receptor Nr4a1 modulates both regulatory T-cell (Treg) differentiation and clonal deletion. *Proc Natl Acad Sci USA* 109:3891–3896.
38. Wu H, et al. (2016) NUR77 exerts a protective effect against inflammatory bowel disease by negatively regulating the TRAF6/TLR-IL-1R signalling axis. *J Pathol* 238:457–469.
39. Li Y, Lau LF (1997) Adrenocorticotropic hormone regulates the activities of the orphan nuclear receptor Nur77 through modulation of phosphorylation. *Endocrinology* 138:4138–4146.